Plasmon-assisted transmission of entangled photons

E. Altewischer, M. P. van Exter & J. P. Woerdman

Leiden University, Huygens Laboratory, PO Box 9504, 2300 RA Leiden, The Netherlands

The state of a two-particle system is said to be entangled when its quantum-mechanical wavefunction cannot be factorized into two single-particle wavefunctions. This leads to one of the strongest counter-intuitive features of quantum mechanics, namely non-locality[1,2]. Experimental realization of quantum entanglement is relatively easy for photons; a starting photon can spontaneously split into a pair of entangled photons inside a nonlinear crystal. Here we investigate the effects of nanostructured metal optical elements[3] on the properties of entangled photons. To this end, we place optically thick metal films perforated with a periodic array of subwavelength holes in the paths of the two entangled photons. Such arrays convert photons into surface-plasmon waves—optically excited compressive charge density waves—which tunnel through the holes before reradiating as photons at the far side[4–7]. We address the question of whether the entanglement survives such a conversion process. Our coincidence counting measurements show that it does, so demonstrating that the surface plasmons have a true quantum nature. Focusing one of the photon beams on its array reduces the quality of the entanglement. The propagation of the surface plasmons makes the array effectively act as a 'which way' detector.

Light can potentially couple to surface plasmons (SPs) if the surface in which the SPs reside shows a periodic structure to satisfy conservation of energy and momentum. The samples that we have studied are two metal hole arrays. Each array is 1 mm × 1 mm, and comprises a 200-nm-thick gold layer (on glass) perforated with a square grid of 200-nm-diameter holes spaced with a 700-nm lattice constant; Fig. 1a inset shows a typical scanning electron microscope picture. This figure also shows transmission spectra of the two arrays, measured with a spectrometer using normally incident white light. We can clearly see the resonances due to excitation of SPs on either of the metal–dielectric boundaries. At these resonances, the measured transmission can be orders of magnitude larger than the value obtained from classical diffraction theory for subwavelength holes[4,8]. In a simple picture, the surprisingly large transmission is due to the coupling of a photon to an SP on one side of the metal, subsequent tunnelling of the SP through the holes to establish an SP at the other side, and final reradiation into a photon[5]. Other prominent features in the spectra are the transmission minima associated with Wood anomalies[6]. The theoretical description of the full transmission spectrum is incomplete at present, but the role of the SP is well established[5–7]. The resonance used in our experiment is centred at 809 nm, and has a width of ~40 nm; a calculation based on the geometry of the array and the optical constants of gold and glass shows that it is associated with the $(\pm1,\pm1)$ SP mode on the glass–metal interface. The label $(\pm1,\pm1)$ denotes any of the four diagonal directions that are frequency degenerate for excitation under normal incidence. Peak transmissions of the two arrays at 813 nm are typically 3% (dashed curve) and 5% (solid curve); these values are much larger than the value of 0.55% obtained from classical theory[8]. The difference in transmission between the two nominally identical hole arrays is ascribed to production imperfections.

Because an SP is a mainly longitudinal, compressive electron density wave, its propagation direction depends on the polarization axis of the incident light, following a certain dispersion relation[9,10]. In order to confirm this for our samples, we have measured polarization-resolved transmission spectra of one of the hole arrays for various angles of incidence θ_{inc} of plane-wave radiation (Fig. 1b and c). Angle tuning is expected to shift the various resonances in the transmission spectrum in different ways. As we have theoretically associated the peak at 809 nm with a $(\pm1,\pm1)$ SP, we have varied the angle of incidence by tilting the samples along the diagonal axis of the square hole array. For incident light polarized orthogonal to this tilting axis (Fig. 1b), the 809-nm peak splits and shifts for increasing θ_{inc}; for incident light polarized along the tilting axis (Fig. 1c), the 809-nm peak remains at approximately the same spectral position. These results confirm the association of the 809-nm peak with the $(\pm1,\pm1)$ SP.

We generate polarization-entangled twin photons at a wavelength of 813 nm with the standard method of type II spontaneous parametric down-conversion[11,12] depicted in Fig. 2. The twin

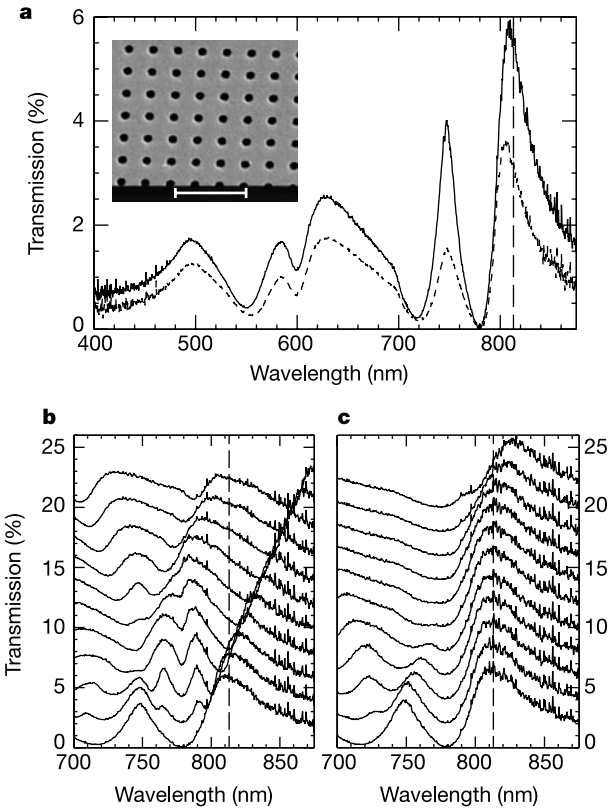

Figure 1 Wavelength-dependent transmission of the arrays used in the experiment. The dashed vertical line indicates the wavelength of 813 nm used in the entanglement experiment. **a**, The transmission of the two arrays. Inset, scanning electron microscope picture of part of a typical hole array. Scale bar, 2 μm. The hole arrays were produced at the Delft Institute of Micro-Electronics and Sub-micron Technology (DIMES) by first defining, with electron beam lithography, arrays of dielectric pillars on a 0.5-mm-thick glass substrate, subsequently evaporating the gold layer onto a 2-nm titanium bonding layer, and finally etching away the pillars to leave the array of air holes. **b**, **c**, Wavelength-dependent transmission of one of the hole arrays for various angles of incidence at a polarization orthogonal to the tilting axis (**b**) and along the tilting axis (**c**). In both graphs the lowest curve is measured with the probe beam at normal incidence, while consecutive curves are measured at increasing angles of incidence (one-degree steps) by subsequent tilting of the square hole array around a diagonal. These curves have been plotted with subsequent vertical offsets of 2% on the transmission scale. The resonance around 813 nm (dashed line) shows a complicated splitting for a polarization orthogonal to the tilting axis (**b**), whereas it is approximately stationary for a polarization along this axis (**c**).

photons travel along two 'beam lines' defined by pinholes, pass through polarizers P1 and P2, and are detected by single-photon counters. The photodetectors act as 'bucket detectors'—that is, they impose no further transverse mode selection (this is only done by pinholes). To provide the two-photon coincidence rate, the signals from the two detectors are combined electronically in a coincidence circuit with a time window of 2 ns.

In a simplified picture, the generated polarization-entangled state is

$$|\Psi\rangle = \frac{1}{\sqrt{2}}(|H_1V_2\rangle + e^{i\theta}|V_1H_2\rangle) \quad (1)$$

where the state $|H_1V_2\rangle$ represents the simultaneous emission and propagation of an H-polarized photon in beam 1 and a V-polarized photon in beam 2. The H- and V-directions are defined by the orthogonal birefringent axes of the BBO (β barium borate) crystal generating the twin photons, and all spatial information is implicitly contained in the beam labelling. By tilting one of the compensating crystals (C in Fig. 2), the quantum phase θ can be set.

In the absence of the hole arrays, our set-up produces typically 3.2×10^4 coincidence counts per second, which is ~25% of the single count rate. A measure for the purity of the quantum entangled state is the so-called visibility of the biphoton fringe[11,12]. This visibility was typically $V_{0°} = 99.3\%$ and $V_{45°} = 97.0\%$ at polarization angles of 0° and 45°, respectively (see Table 1). The high value at 45° shows that the natural preference of the BBO crystal for its birefringent axes (0° and 90°) was almost completely removed in our set-up by the compensating crystals C, which act as quantum erasers.

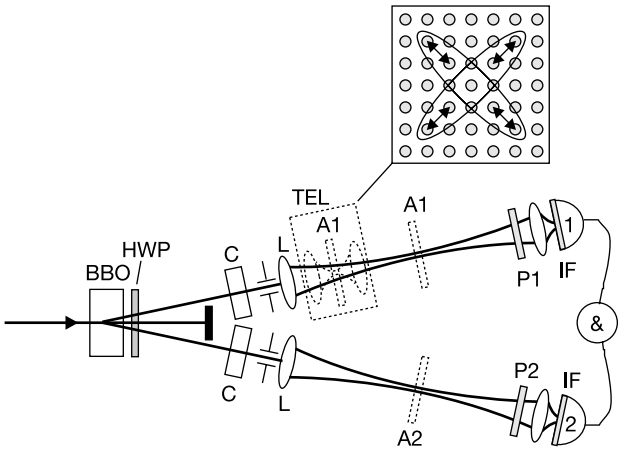

Figure 2 Experimental set-up. A 240-mW continuous-wave krypton-ion laser beam at a wavelength of 406.7 nm is directed onto a 1-mm-thick BBO nonlinear crystal, where the beam diameter is ~0.50 mm (full width at $1/e^2$ points). Inside the nonlinear crystal, a small fraction of the pump photons is down-converted into twin photons at the doubled wavelength (813 nm); these are emitted along two intersecting cones. Polarization-entangled photon pairs are selected with pinholes at the crossings of these cones; the size of the pinholes (far-field diameter 5 mrad) was chosen as a compromise between high yield and good quantum entanglement. Lenses L of 40 cm focal length produce a one-to-one intermediate image of the pumped area, which is used in some experiments to accommodate the hole arrays A1 and A2. After passing through polarizers P1 and P2, the entangled twin photons are focused through interference filters IF (10-nm bandwidth centred at 813 nm) onto single-photon counting modules (Perkin Elmer SPCM-AQR-14). Beam walkoff is compensated by the standard quantum eraser comprising a half-wave plate HWP at 45° and compensating crystals C with a thickness equal to half of that of the generating crystal[11,12]. The dotted objects are present only in some experiments; they show the hole arrays A1 and A2 at the image positions created by lenses L, or, alternatively, in the focus of the confocal telescope TEL (15 mm focal length lenses). Inset, schematic picture of the near field at the back of array A1 when this is positioned inside the telescope. The arrows indicate the polarization direction of the optical electric field; the centre region is unpolarized.

Placement of the two hole arrays in the two beam lines leads naturally to a marked reduction of single and coincidence counts. Coincidence count rates are typically $55\,s^{-1}$ at the optimum setting of the detecting polarizers, which is consistent with the transmissions of the arrays given above ($3\% \times 5\% \times 3.2 \times 10^4\,s^{-1} \approx 50\,s^{-1}$). We again measured the purity of the entangled state, and found that the visibilities were now $V_{0°} = 97.1\%$ and $V_{45°} = 97.2\%$, respectively. In Fig. 3 the corresponding fourth-order quantum interference fringes are shown for polarizer P2 fixed at 0° and 45°, and P1 varying in steps of 10°. These measurements show convincingly that the quantum entanglement almost completely survives the transition from photon to SP and back. As a further confirmation, we performed a measurement of the so-called *S*-parameter, as described in ref. 11, on a singlet Bell state ($\theta = \pi$ in equation (1)). This experiment, which took 16 runs of 100 seconds each, gave a value of $|S| = 2.71 \pm 0.02$, which is a violation of the classical inequality ($|S| \leq 2$; ref. 13) by 35 standard deviations.

Further experiments were done on a set-up with only a single array in one of the beams. The results for this case look very similar to those for the experiment with two arrays; again the entanglement was practically unaffected (see Table 1). This is to be expected, as the two-photon wavefunction of equation (1) is perturbed by changes in either of its single-photon components; in principle, a single array could have removed all entanglement. The difference between the two single-array experiments (Table 1) is due to imperfections in array 2, which are also observable in its (single-photon) polarization-dependent transmission. As the measurements using only array 2 gave results very similar to the situation with both arrays in place, these imperfections must have caused the somewhat limited visibilities in the two-array experiment.

The most intriguing results of our single-array experiment are obtained when we focus one of the beam lines onto its hole array, using a confocal telescope (close to lens L) of two $f = 15$ mm lenses symmetrically positioned around the array, as shown inside the large dotted rectangle in Fig. 2. Under these conditions, we observe a notable reduction of the degree of quantum entanglement: when the intra-telescope focus has a numerical aperture of 0.13, we observe visibilities of $V_{0°} = 73\%$ and $V_{45°} = 87\%$ (Table 1).

The observed reduction in visibility on focusing can be explained as a consequence of the non-local relation between the electronic excitation in the metal film and the incident optical field; SPs are not at all local, but instead propagate along the dielectric–metal interface at nearly the speed of light over distances of many optical wavelengths[3,9,10]. As a result of this propagation, the near-field distribution of the photons that are reradiated at the back of the hole array differs from the spatial profile of the 'polarization-isotropic' incident photons. Because we use the $(\pm1,\pm1)$ SP resonance (at 809 nm) we expect—for unpolarized incident light—a near-field pattern consisting of two orthogonal 'ellipses' at the back of the hole array (Fig. 2 inset). The unpolarized overlap region of these ellipses correspond to the focused incident light, whereas the polarized 'protuberances' introduce the possibility of distinguishing the polarization of the photons on the basis of their

Table 1 Biphoton fringe visibilities

Experiment	R (s^{-1})	$V_{0°}$ (%)	$V_{45°}$ (%)
No arrays	32×10^3	99.3	97.0
Both arrays	55	97.1	97.2
Only array 1	1.6×10^3	99.4	97.1
Only array 2	1.0×10^3	97.5	96.8
Array 1, focussed	1.1×10^3	73	87

R, measured coincidence count rate; $V_{0°}$ and $V_{45°}$, measured visibility for one of the polarizers fixed at 0° and 45°, respectively.

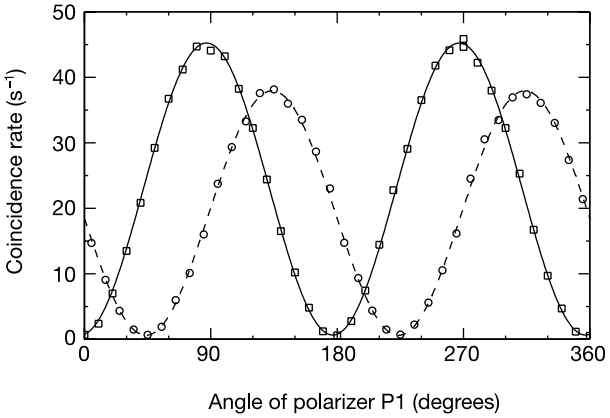

Figure 3 Biphoton fringes. These fringes correspond to fourth-order quantum interference, and were measured with the two hole arrays in place, for P2 fixed at 0° (solid curve) and 45° (dashed curve), and P1 varying in steps of 10°.

spatial near-field coordinates. This will then automatically remove part of the polarization entanglement, just as any 'which way' information will do. Note that the observed reduction in visibility is much stronger for $V_{0°}$ than for $V_{45°}$, contrary to what is generally found without using hole arrays[11,12]. This observation is consistent with the fact that we excite SPs propagating in the 'diagonal' (45°) directions.

The non-local nature of the electronic response is equivalent to an explicit wavevector dependence of the dielectric function ('spatial dispersion'; ref. 14). The latter description highlights the far-field aspects of a non-local dielectric response, and is related by way of a Fourier transform to the near-field picture given above.

A theory for the reduction of visibility due to this effect must intrinsically be a multimode theory because, after passage through the hole arrays, the spatial information within each beam should be accounted for. Discussion of such a theory is beyond the scope of this Letter, but qualitative arguments are easily found. When adopting a near-field point of view, the reduction of the visibility is expected to be significant when the propagation or coherence length l of the SP is comparable to the transverse coherence length of the focused incident beam. This is indeed the case for our experiment: on the basis of the spectral width of the transmission peak at 809 nm, we estimate $l \approx 4\,\mu$m; the number of holes 'covered' by the propagating SPs is thus about 10. In comparison, the transverse coherence length of the light is $\sim 4\,\mu$m (set by the 5-mrad far-field selection due to the pinholes; Fig 2). We note that the SP propagation length is an order of magnitude smaller than the value $l \approx 40\,\mu$m predicted for a smooth pure gold film[3]; we ascribe this difference to radiative decay due to the hole patterning, and to extra damping by the titanium bonding layer.

From a general perspective, the observed conservation of quantum entanglement for the conversion from photon → surface plasmon → photon is a demonstration of the true quantum nature of SPs. All experiments on SPs so far have not probed their quantum nature, but only their wave nature through their semiclassical dispersion relation. We note that the true quantum nature of the photon was only established in 1977, in anti-bunching experiments[15,16]. Furthermore, a simple estimate shows that SPs are very macroscopic, in the sense that they involve some 10^{10} electrons. Our experiment proves that this macroscopic nature does not impede the quantum behaviour of SPs, because they can act as intermediates in transmitting entangled photons to yield the expected fourth-order interference.

A theory for our experiments based only on locally induced surface currents is clearly inadequate. We stress this point because some recent theoretical models for one-dimensional gratings in thick metal films have questioned the role of SPs, emphasizing instead waveguide effects. Our arrays are apparently thin enough (thickness/period ≈ 0.3) for waveguide effects not to play an important role. This conclusion is supported by experiments in which the thickness of such a 'thin' array has been varied[6].

By addressing the topic of plasmon-assisted transmission of quantum entangled photons, we have combined two fields of research, namely quantum information and nanostructured metal optics. We hope that our work will stimulate other studies of the transfer of entanglement to condensed-matter degrees of freedom. □

Received 11 March; accepted 23 May 2002; doi:10.1038/nature00869.

1. Greenberger, D. M., Horne, M. A. & Zeilinger, A. Multiparticle interferometry and the superposition principle. *Phys. Today*, 22–29 (August 1993).
2. Bouwmeester, D. *et al.* Experimental quantum teleportation. *Nature* **390,** 575–579 (1997).
3. Raether, H. *Surface Plasmons* (Springer, Berlin, 1988).
4. Ebbesen, T. W., Lezec, H. J., Ghaemi, H. F., Thio, T. & Wolff, P. A. Extraordinary optical transmission through sub-wavelength hole arrays. *Nature* **391,** 667–669 (1998).
5. Martin-Moreno, L. *et al.* Theory of extraordinary optical transmission through subwavelength hole arrays. *Phys. Rev. Lett.* **86,** 1114–1117 (2001).
6. Ghaemi, H. F., Thio, T., Grupp, D. E., Ebbesen, T. W. & Lezec, H. J. Surface plasmons enhance optical transmission through subwavelength holes. *Phys. Rev. B* **58,** 6779–6782 (1998).
7. Grupp, D. E., Lezec, H. J., Ebbesen, T. W., Pellerin, K. M. & Thio, T. Crucial role of metal surface in enhanced transmission through subwavelength apertures. *Appl. Phys. Lett.* **77,** 1569–1571 (2000).
8. Bethe, H. A. Theory of diffraction by small holes. *Phys. Rev.* **66,** 163–182 (1944).
9. Hecht, B., Bielefeldt, H., Novotny, L., Inouye, Y. & Pohl, D. W. Local excitation, scattering, and interference of surface plasmons. *Phys. Rev. Lett.* **77,** 1889–1892 (1996).
10. Sönnichsen, C. *et al.* Launching surface plasmons into nanoholes in metal films. *Appl. Phys. Lett.* **77,** 140–142 (2000).
11. Kwiat, P. G. *et al.* New high-intensity source of polarization-entangled photon pairs. *Phys. Rev. Lett.* **75,** 4337–4341 (1995).
12. Kurtsiefer, C., Oberparleiter, M. & Weinfurter, H. High efficiency entangled photon pair collection in type II parametric fluorescence. *Phys. Rev. A* **64,** 023802-1–023802-4 (2001).
13. Clauser, J. F., Horne, M. A., Shimony, A. & Holt, R. A. Proposed experiment to test local hidden-variable theories. *Phys. Rev. Lett.* **23,** 880–884 (1969).
14. Landau, L. D., Lifshitz, E. M. & Pitaevskii, L. P. *Electrodynamics of Continuous Media* 2nd edn (Pergamon, Oxford, 1984).
15. Lu, Y. J. & Ou, Z. Y. Observation of nonclassical photon statistics due to quantum interference. *Phys. Rev. Lett.* **88,** 023601-1–023601-4 (2002).
16. Kimble, H. J., Dagenais, M. & Mandel, L. Photon antibunching in resonance fluorescence. *Phys. Rev. Lett.* **39,** 691–695 (1977).

Acknowledgements

We thank A. van Zuuk and E. van der Drift for the production of the hole arrays, and G. Nienhuis for theoretical discussions. This work was supported by the Stichting voor Fundamenteel Onderzoek der Materie (FOM), and the European Union under the IST-ATESIT contract.

Competing interests statement

The authors declare that they have no competing financial interests.

Correspondence and requests for material should be addressed to E.A. (e-mail: erwin@molphys.leidenuniv.nl).